# Reduction of back-trap mottle through optimization of the drying process for paper coatings, part I

LINDA H. KIM, MARK J. POLLOCK, EDWARD L. WITTBRODT,
JOHN A ROPER, III, DAVID A. SMITH, JOHN W. STOLARZ,
MICHAEL J. ROLF, TERRELL J. GREEN, AND BARBARA J. LANGOLF

## ABSTRACT

*The drying of paper coatings can significantly affect the back-trap mottle of coated paper. This study identified an optimum drying strategy for a mill and the best latex binder to reduce back-trap mottle by preparing samples on a pilot coater under different drying conditions and printing on a commercial six-color press. Computer modeling helped to understand the critical drying process parameters and to translate the pilot coater results to the drying process of the mill. Results shows the important variables influencing back-trap mottle. Back-trap mottle is very sensitive to drying conditions near the first critical concentration drying zone. X-ray photoelectron spectroscopy data showed no significant differences in the distribution of surface components between samples with good mottle and poor mottle. Drying conditions did not significantly affect coating properties other than back-trap mottle.*

***Application:***

*Drying strategy, binder type, coating weight, and IR drying and coating speed influence back-trap mottle.*

THE PRIMARY OBJECTIVES OF this study were identification of the optimum drying strategy for a mill and the best latex binder to reduce back-trap mottle. Samples prepared on a pilot coater used a variety of drying strategies. Printing of these samples used a commercial six-color press to determine the impact of drying on back-trap mottle. A Thurstone all pairs comparison ranking generated a numerical scale for mottle to evaluate subtle differences in mottle.

Another study objective was to better understand the mechanisms that cause back-trap mottle. Believing that different drying strategies would lead to different degrees of binder migration, we used scanning electron microscope (SEM) micrographs and X-ray photoelectron spectroscopy (XPS) data to help quantify binder migration. In addition, cryo-SEM micrographs of the wet coating colors helped to understand the effect of latex on the degree of dispersion in the wet coating structure and its impact on coating consolidation during drying. This study incorporated three latex binders that show different sensitivities to drying conditions in a mill.

Back-trap mottle is a common problem in offset printing especially in sheet fed operations. It is often the primary determinant of subjective print quality. Multiple impression mottle is another term for back-trap mottle. It occurs as random, unintended variations in color reflectance of transparent process colors that undergo contact with subsequent blankets. Back-trap mottle is due to the uneven permeability of a coating toward ink diluent. Surface uniformity and control of its variation are therefore key considerations. Initial nonuniformities in the original coating before application and any subsequent redistribution of coating constituents during consolidation of the coating layer can affect surface uniformity.

Factors that influence back-trap mottle include basestock formation, choice of pigments, choice of binders, and the drying process. Control of back-trap mottle is necessary because of the continually increasing demands for improved print quality by printers. A further understanding of the mechanisms that cause back-trap mottle would help to optimize coating conditions and binder choices to obtain the highest quality paper possible.

The term mottle will pertain only to back-trap mottle in the remainder of this paper.

Structure and chemical composition of a coating layer influence its evenness and resultant print quality. The source of a nonuniform surface is often attributed to uneven binder distribution in the coating surface due to binder migration based on indirect stain tests. An inappropriate drying strategy can often cause binder migration. An uneven web structure or coating can further exacerbate this. Many studies on the impact of drying conditions on mottle are available *(1–6)*. The effect of binder type on mottle has had less study than the effect of drying. One report did indicate that binder type can influence mottle as much as drying *(7)*.

Current industry understanding acknowledges the existence of a critical drying zone within which evaporation rates require restriction to maintain print quality (8–14). Reduction of evaporation rates within this zone to below some threshold value will usually reduce mottle (15). Differences in migration can only occur during this critical zone. These differences can result in significant variations of print quality. Papers coated with the same coating on the same basestock with the same coating weight can exhibit a wide range of mottle depending on what occurred

| Coating | Binder Tg | Binder particle size | Binder carboxylation |
|---|---|---|---|
| A | Low | Large | Medium |
| B | High | Small | Medium |
| C | Medium | Medium | Low |

*I. Description of coatings A, B, and C*

| Coating | Solids, % | pH | Brookfield viscosity, 100 rpm, mPa | Static dewatering rate, g/m² |
|---|---|---|---|---|
| A | 64.9 | 8.5 | 2060 | 147 |
| B | 65.1 | 8.6 | 1570 | 137 |
| C | 65.0 | 8.6 | 1800 | 131 |

*II. Data for pilot coater coating colors*

| Run Number | Air setpoint temperatures, °C D1 | D2 | D3 | D4 |
|---|---|---|---|---|
| A1 | 232 | 232 | 38 | 38 |
| A2 | 149 | 149 | 149 | 149 |
| A3, B3, C3 | 38 | 38 | 232 | 232 |
| A4 | 107 | 107 | 204 | 204 |
| A5 | 204 | 107 | 107 | 204 |
| A6, B6, C6 | 204 | 107 | 204 | 107 |
| A7, B7, C7 | 107 | 204 | 107 | 204 |
| A8 | 107 | 204 | 204 | 107 |
| A9, B9, C9 | 204 | 204 | 107 | 107 |

*III. Drying profiles on the pilot coater*

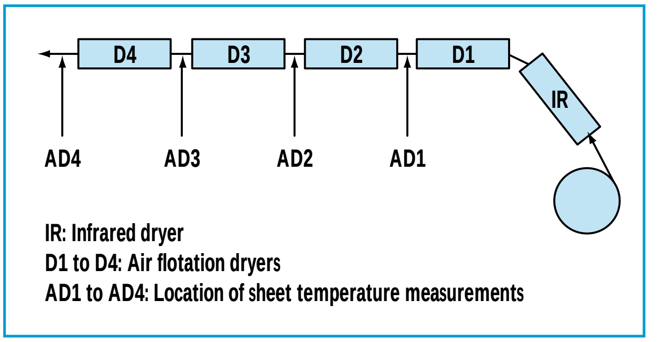


*1. Schematic of pilot coater dryers*

within the critical drying zone. The critical coating solids range corresponding to this zone is approximately 59–75% where the coating starts to consolidate and approximately 81–90% where total immobilization occurs. These values depend on formulation factors. Increased drying rates before coating immobilization is desirable with reduced drying rates in the critical zone to reduce binder migration that can lead to mottle. After total coating immobilization, the drying rates do not significantly affect coating quality.

Although this general drying strategy is common, its application in a particular mill is difficult because of the uncertain location of the critical drying zone. The critical drying zone is sensitive to the initial moisture content of the coating, how much water has dewatered into the sheet, and the evaporation rates employed *(15)*. After application of the coating, there is an initial surge of water into the basestock. Delaying the start of evaporation results in drawing more water into the basestock. The ratio of drained water to evaporated water will affect the position and nature of the immobilization point. One suggestion is that this basestock absorption causes swelling of fibers and water-induced roughening *(9)*. These cause differential mass distribution of the coating layer.

Data generated on a pilot coater may not readily translate to the mill environment because of differences in dryer configuration. We applied computer modeling to the drying process for two reasons. One was to develop a better understanding of how drying variables affect the susceptibility of the coatings to mottle. The other was to translate the pilot coater results to the mill by calculating the critical drying zone from mill process control data. Although software programs are available to design and optimize the drying process, the problem has been to obtain reliable input data. In this study, we systematically varied drying conditions to cover a range of drying strategies for inclusion in the computer modeling.

## EXPERIMENTAL

### *Materials*

The basis weight of the wood-free base paper in this study was 112 g/m² (74 lb/ream). The coating formulation had 57 parts of a No. 1 high brightness clay, 43 parts of an ultrafine calcium carbonate, 15.3 parts of styrene/butadiene latex binder, and 0.40 parts of a carboxymethylcellulose thickener. Coating solids was 65%. Coatings A, B, and C used the three binders shown in **Table I**.

Binder selection included a high glass transition temperature and small particle size product that would be more conducive to binder migration and a low glass transition temperature and large particle size binder that would be less conducive to binder migration *(16, 17)*.

### *Wet coating characterization*

***Cryofixation.*** Plunging a small drop of the paper coating color on a hollow copper sample trivet into liquid nitrogen rapidly froze the sample. We transferred the frozen sample to a precooled (-130°C) Oxford CT 1500 cryo-preparation vacuum chamber and increased the temperature of the sample to -90°C. Fracturing the sample with a precooled scalpel blade exposed a fresh face that we held at the temperature for 2 min to sublime the surface ice.

We sputtered a thin layer of conductive gold onto the samples while they were in the cryo chamber and then transferred them directly into an attached JSM-6320FV field emission gun SEM for examination at -120°C.

***Consolidation.*** We recorded gloss and weight loss measurements vs. time. The coatings were applied on plastic Leneta scrub test panels fol-

| Variable | Description |
|---|---|
| Z1 temperature | Zone 1 temperature |
| Z3 temperature | Zone 3 temperature |
| Delta T1 | Difference in sheet temperature from the start of zone 1 to the end of zone 2 |
| Delta T2 | Difference in sheet temperature from the start of zone 2 to the end of zone 3 |
| Start temperature | Distance in dryer section at which sheet temperature first starts to drop due to evaporative cooling |
| CS range | Time in the dryer section during the transition through the critical solids range (72–81% coating solids) normalized by coating weight |
| Avg ER | Average evaporation rate in the critical solids zone |
| Max ER | Maximum evaporation rate in the critical solids zone |
| Delta ER | Differential in evaporation rate from the start to the end of the critical solids zone |
| ER at 23.5% | Evaporation rate at the center of the critical solids zone moisture |
| Coating weight | Coating weight |
| Latex | Latex type normalized by Thurstone scale ratings within the drying conditions of the latex evaluation |
| Speed | Web speed |

*IV. Input variables for regression analysis*

lowed by measurement of 75° gloss with time using a Hunter glossmeter as the coatings dried at room temperature. Weight loss was continuously measured with time to calculate the coating solids.

### *Pilot coater conditions*

***Pilot coater.*** **Figure 1** shows a schematic of the pilot coater dryers for this study. They consisted of infrared dryers followed by four air flotation dryers. (Note the absence of dryer cans.) A series of infrared pyrometers provided sheet temperature measurements at positions AD1, AD2, AD3, and AD4. (Note that A is the designation for after, and D is the designation for an air flotation dryer with its number.)

***Coating conditions.*** We coated the coating colors on two sides on the pilot coater at 884 m/min (2900 ft/min). A flooded nip applicator unit had a 0.508-mm (0.020-in.) blade with a 45° angle. Application temperature of the coating colors was 30°C. Adjustment of the blade pressure achieved the coating weight target of 19 g/m$^2$ (13 lb/ream). **Table II** shows data for the coating colors. The Abo Akademi AA-GWR test apparatus *(18)* using 0.5-atm pressure for 2 min determined the static dewatering rate of the coating colors.

***Drying strategy.*** The drying study had four parts. In the first data subset, coating A—the control—underwent the wide range of drying profiles in **Table III** to span a wide mottle range. The columns labeled D1, D2, D3, and D4 refer to the air setpoint temperatures for the four air flotation dryers. The extreme drying conditions defined by run A1 represented harsh-early followed by mild-late drying and those of run A3 represented mild-early followed by harsh-late drying. Run A2 used a moderate drying profile. The remaining drying profiles were intermediate drying conditions with the dryer temperatures varied systematically for subsequent optimization purposes. The nozzle air pressures for a given air flotation dryer remained constant so nozzle velocities varied with air setpoint temperatures.

Note that A, B, and C in the run number nomenclature refer to the binders of Table I. For the second data subset, four conditions' drying profiles A3, A6, A7, and A9 were identical to the first study for coatings B and C. These drying profiles covered the range of mottle results seen in the first subset. These same four conditions evaluated the effect of lower coating weight 13 g/m$^2$ (9 lb/ream) for coating A in the third data subset. XPS and cryo-SEM analyses were done on coatings from the second subset of coating conditions because they spanned the range of mottle behavior. Evaluation of the use of infrared drying and changes in coating speed 975 m/min or 3200 ft/min used only limited runs in the fourth data subset because the major focus of this study was on variation of the air flotation drying profile.

***Finishing conditions.*** The coated papers underwent supercalendering at 3 x 107 g/m$^2$ and 93°C using four nips per side at 305 m/min (1000 ft/min). We then sheeted these papers and printed them on a six-color sheet fed press.

### *Coated paper characterization*

***SEM.*** We sectioned representative samples of the coated papers and stained them with osmium tetraoxide for 24 h. The samples then underwent impregnation with an epoxy resin impregnated in a vacuum followed by pressure curing overnight and polishing. A Cambridge S-360 SEM provided back scattered electron imaging.

***XPS.*** A Kratos AXIS 165 X-ray photoelectron spectrometer provided XPS spectra. Line profile measurements used 11 sample points at 1-mm increments. Each data point represents a 200 µm x 600 µm area. Element peaks used for determining the components were the following: Na (1s), O (1s), Ca (2p), C (1s), Si (2p), and Al (2p).

***End-use testing.*** End-use testing used TAPPI test method procedures.

### *Press trial protocol*

***Make ready.*** Plates in the six-color sheet fed press had the following sequence: black, cyan, magenta, yellow, black, and cyan. The press design in-

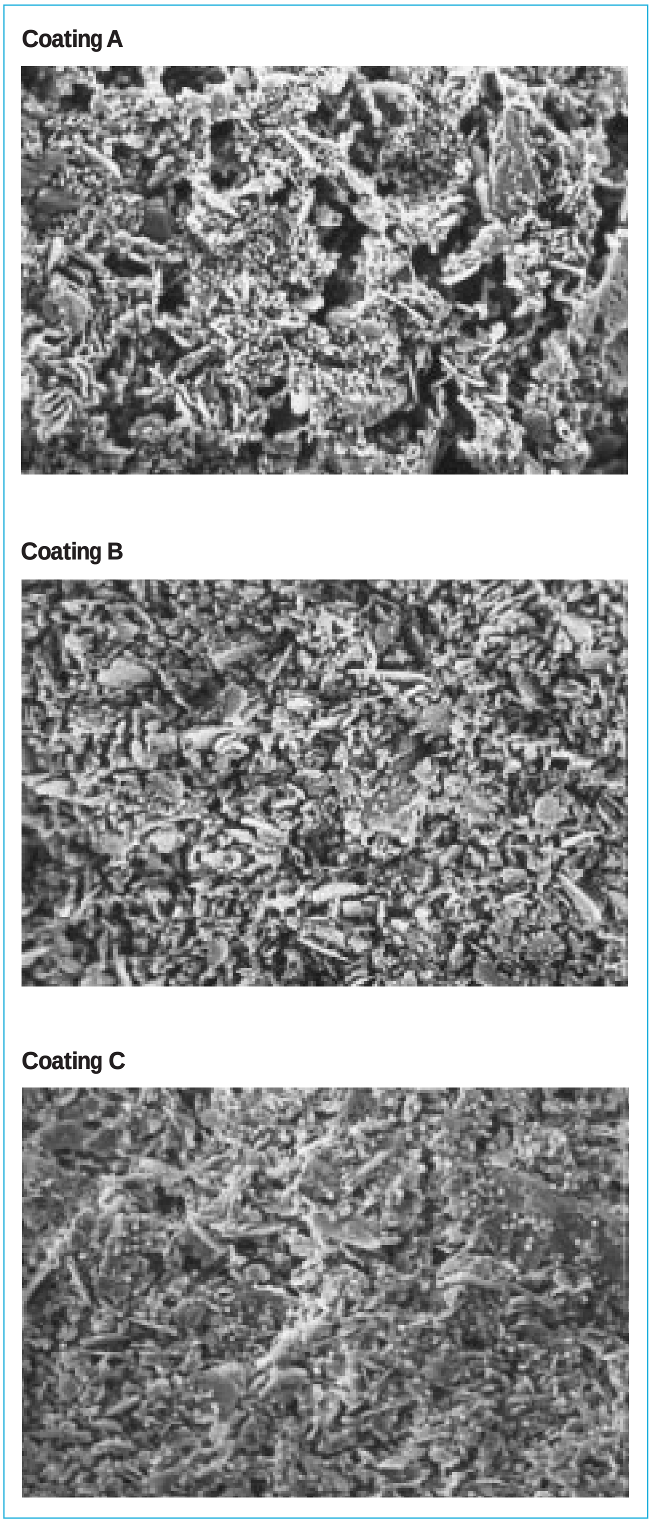


2. Cryo-SEM of coatings A, B, and C

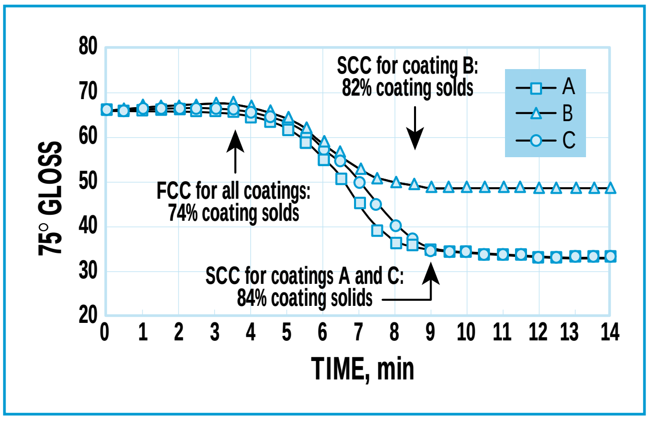


*3. Gloss measurements of the coatings with time*

corporated bearer to bearer contact between the blanket cylinder and impression cylinder. Blanket to paper impression was set by packing blanket 0.1 mm (0.004 in.) over the bearer. All units used the same brand and concentration of one step alcohol-free fountain solution. The pH was 4.2, and the electrical conductivity was 1300– 1500 micro Siemens.

The lift contained house paper that was close in caliper and quality to the test paper. This allowed ink densities and registration to come close to the specified range. After starting the press, we adjusted the ink and fountain solution flow to prevent catch up and to ensure that the tiny, 4% unprinted circles in a 96%, 150 lines per in. (59 lines per cm) shadow tone were open. Press speed was 8000 impressions per hour. Solid, 100%, ink densities were within 0.05 density units of the specified targets: black 1.55, cyan 1.20, magenta 1.20, and yellow 0.90.

***Test print run.*** After the press operator was satisfied with the ink and fountain solution balance, we loaded the lift with 500 sheets of each test paper. We loaded 500 sheets of house paper last to run first to allow for final adjustment of ink densities. Then we restarted the press at the same speed.

After running 200 sheets, we pulled a bundle of 20 sheets and carefully stapled them together to prevent scuffing during shipping. If any problems arose after 200 sheets, we made appropriate adjustments, ran an additional 200 sheets and pulled 20 more sheets.

***Distinguishing back-trap mottle from other mottle.*** To avoid confusion with various types of halftone mottle, we restricted the subjective evaluations to the 200% secondary blue trap formed by 100% second down cyan and 100% third down magenta. After this wet trap occurred on the press, three further back-trapping contacts were imposed on the ink films through the design of the print form and color sequence.

To avoid confusion with wet repellency mottle, we made comparisons between the 100% second down cyan and the 100% sixth down cyan. If wet repellency had occurred, it would have been a light, sometimes grainy mottle in late unit colors.

***Ranking and rating of mottle***

We visually evaluated mottle of the print signatures in an all-pairs comparison ranking of the samples separated into the four data subsets. A Thurstone scale factor for the mottle rankings assessed the relative intensities of perceived print quality differences *(19, 20)*. This Thurstone scaling generat-

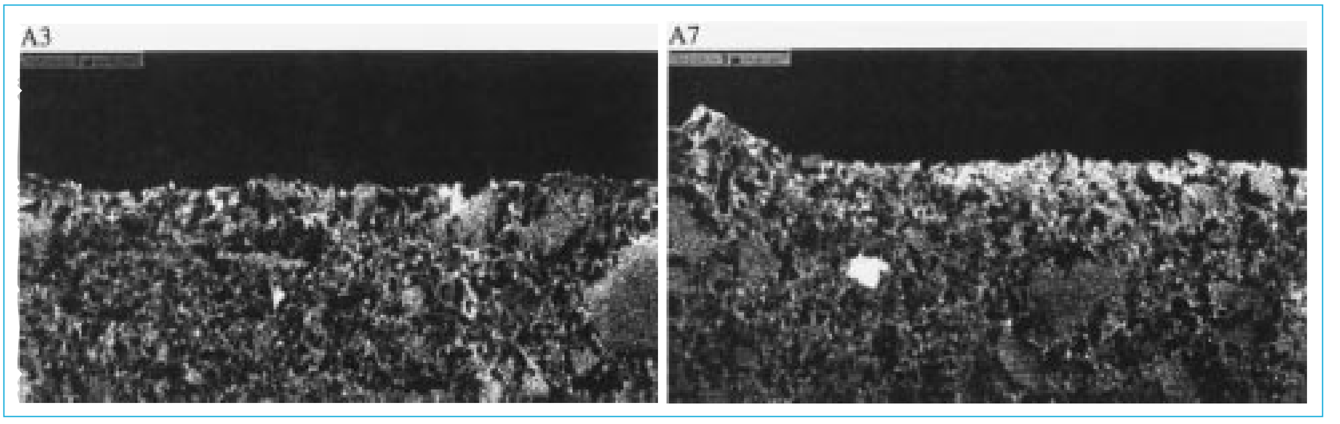


*4. Cross-sectional SEM of A3 and A7*

ed a linear numerical scale to distinguish subtle differences in mottle and related the magnitude of the data to a proportion of the population. A lower Thurstone scale factor correlates to samples exhibiting less mottle. We also generated Thurstone scale ratings from the combined data of all four data subsets.

### Statistical analysis and computer modeling of the drying process

***Statistical analysis.*** We initially used 13 independent variables for a regression analysis with the composite Thurstone mottle ratings as the response. **Table IV** shows these variables selected using mill experience.

We disregarded input variables that were highly confounded with each other or showed low sensitivity defined as the product of the regression coefficient of a variable with its range of values. We also conducted a factor analysis using linear combinations of the above input variables with the Thurstone scaling values.

***Computer modeling.*** A proprietary software program from TEC Systems modeled the drying process. The following eight input variables were necessary: pilot coater geometry (sheet path distances), coating speed, coating weight, initial basestock and coating moisture content, dryer setpoint temperature, nozzle velocity, and humidity of the ambient air. We did not monitor recycle moisture. The output data consisted of the calculated net evaporation rates, sheet temperatures, and moisture content for the coatings throughout the drying process.

## RESULTS

### Wet coating characterization

***Cryofixation.*** We examined the wet coatings using cryofixation and SEM to assess the state of dispersion before coating application. This technique allows the study of microstructures in coatings *(21)*. Cryo-SEM looked for evidence of latex effects on the degree of dispersion in the wet coating structure and its possible impact on coating consolidation during drying.

**Figure 2** shows the cryo-SEM results at 12,500X magnification. The data indicate more open structures for coating A than the other coatings. Although the differences between coatings B and C were more subtle, coating C exhibits a more consistent distribution of wet state microstructure. The initial wet coating microstructure or its sensitivity to immobilization under super cooled conditions may relate to the susceptibility for mottle.

***Coating consolidation.*** Watanabe and Lepoutre *(22)* have proposed a mechanism for structure consolidation during drying. They defined two structural parameters—the first critical concentration (FCC) and the second critical concentration (SCC). The FCC represents the immobilization point where a pigment matrix has developed in the wet coating layer and particle alignment at the surface is maximum. The water film at the coating surface breaks at the FCC. This corresponds to a decrease in gloss. Menisci start to form at the surface of the wet coating as drying continues. Coalescence of the binder in the presence of water occurs between the FCC and SCC. This results from the development of capillary forces that draw the matrix together. The particle network compacts until sufficiently tight to resist the compressive forces at the SCC. This is the point of maximum compaction and represents the solids concentration of maximum packing. After the SCC, air replaces the remaining water left in the pores corresponding to an increase in opacity.

**Figure 3** shows the immobilization curves of all the coatings. The curves indicate that the FCC of all the coating layers occurred at a coating solids content of approximately 74%. The SCC occurred at a coating solids content of approximately 82% for coatings A and C and approximately 84% for coating B. Delta gloss difference between the initial and final gloss measurements was significantly smaller for coating B than for coatings A and C. The smaller delta gloss and smaller SCC values exhibited by coating B were normal because of the higher glass transition temperature of binder B.

### Effect of drying strategy on mottle

The primary objective of this study was identification of the critical drying process parameters to reduce mottle for a mill. Drying strategy and binder type were the only variables from the

| Run Number | Air setpoint temperatures, °C D1 | D2 | D3 | D4 | TSF |
|---|---|---|---|---|---|
| A7R | 107 | 204 | 107 | 204 | 0.00 |
| A7 | 107 | 204 | 107 | 204 | 0.39 |
| A5 | 204 | 107 | 107 | 204 | 0.58 |
| A1R | 232 | 232 | 38 | 38 | 0.91 |
| A2 | 149 | 149 | 149 | 149 | 1.05 |
| A1 | 232 | 232 | 38 | 38 | 1.32 |
| AIR1 | 204 | 204 | 107 | 107 | 1.55 |
| A9 | 204 | 204 | 107 | 107 | 1.66 |
| A4 | 107 | 107 | 204 | 204 | 1.98 |
| A8 | 107 | 204 | 204 | 107 | 2.45 |
| A6 | 204 | 107 | 204 | 107 | 2.49 |
| A3 | 38 | 38 | 232 | 232 | 2.50 |

TSF:Thurstone scale factor

*V. Back-trap mottle for coating A with different drying profiles with best ranking for mottle listed at top*

| Run Number | Air setpoint temperatures, °C D1 | D2 | D3 | D4 | TSF |
|---|---|---|---|---|---|
| C7 | 107 | 204 | 107 | 204 | 0.00 |
| B7 | 107 | 204 | 107 | 204 | 0.09 |
| B9 | 204 | 204 | 107 | 107 | 0.58 |
| A7 | 107 | 204 | 107 | 204 | 0.80 |
| C9 | 204 | 204 | 107 | 107 | 0.85 |
| C6 | 204 | 107 | 204 | 107 | 0.94 |
| C3 | 38 | 38 | 232 | 232 | 1.47 |
| B6 | 204 | 107 | 204 | 107 | 1.76 |
| A9 | 204 | 204 | 107 | 107 | 1.80 |
| A3 | 38 | 38 | 232 | 232 | 2.23 |
| A6 | 204 | 107 | 204 | 107 | 2.42 |
| B3 | 38 | 38 | 232 | 232 | 2.71 |

*VI. Back-trap mottle showing effect of binder type with best ranking for mottle listed at top*

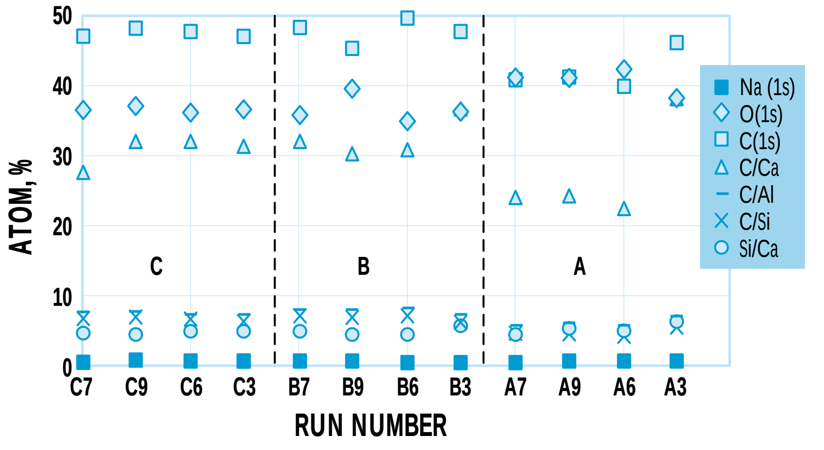


*5. XPS analysis*

four data subsets—drying strategy, binder type, coat weight, and IR drying and coating speed that showed a significant effect on mottle. Further discussion will focus on the effect of these two variables on mottle.

**Table V** shows the mottle ratings of coating A run with different drying profiles. A lower Thurstone scale factor correlates to the least mottle. We replicated sample runs A1 and A7 identified by an R in the run number. The difference in Thurstone scale factors among these replicate runs was approximately 0.40. Sample run numbers A8, A6, and A3 exhibited the most severe mottle and showed similar ratings to each other of approximately 2.50 ± 0.05.

***SEM.*** **Figure 4** shows cross-sectional SEM data of samples A3 and A7. Both samples exhibited a higher binder concentration at the coating surface than at the interior of the coating. Sample A3 showed clustering of the binder at the surface, but sample A7 exhibited a more uniform binder distribution at the surface and a higher binder concentration at the top of the coating surface than sample A3.

### *Effect of binder type on mottle*

**Table VI** shows the mottle ratings of coatings A, B, and C run with four different drying profiles. The effect of drying profiles on mottle for a given binder formulation was consistent. These coatings also had differentiation in their resistance to mottle. The severity of mottle depended on the choice of binder type in the coating formulation as the following average Thurstone scale factors—best to worst—show: 0.82 for coating C, 1.29 for coating B, and 1.81 for coating A.

***XPS.*** We conducted surface characterization by XPS of the coatings to probe the mechanism relating drying conditions to mottle further. Other researchers have used the method to characterize the surface of coated paper (*23–27*). **Figure 5** shows atomic composition defined as the average of 11 points sampled along a line at 1-mm increments.

Coating C exhibited a more consistent distribution of the surface components compared with the other coatings. This provides confirmation of the end-use data that also indicated coating C was the most resistant to mottle. The ratio of C/Ca suggests that increased binder content at the surface resulted only when using a harsh-late drying profile of 38°C, 38°C, 232°C, and 232°C setpoint temperatures for D1, D2, D3, and D4, respectively, for coatings A and B. The ratio of Si/Ca also increased for the harsh-late drying profile indicating higher clay to calcium carbonate ratios. Other than these observations no significant trends based on the standard deviation values of the elemental analysis correlated drying conditions to surface composition, although other cases of significant variations in mottle did occur. For example, samples A7 and A9

| Critical coating solids range | 72–81% | 72–78% |
|---|---|---|
| Delta T2 | 3.08 | 1.09 |
| Delta ER | -2.31 | NA |
| Binder type | 1.26 | 1.34 |
| CS range | -1.16 | NA |
| Max ER | NA | 2.12 |
| R2 | 0.82 | 0.83 |

NA: not applicable

*VII. Sensitivity of significant variables resulting from regression analysis*

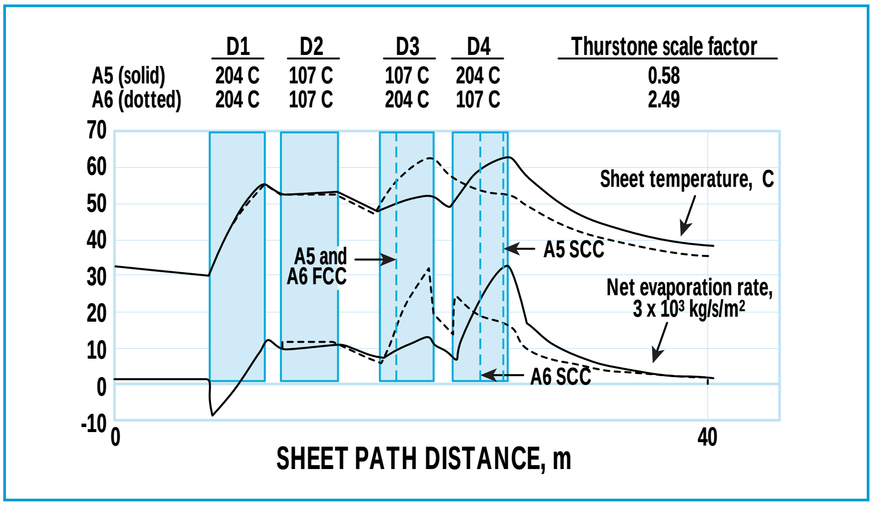


*6. Computer modeling results for A5 and A6 with shaded areas representing air flotation dryers D1–D4*

exhibited significant differences in mottle Thurstone scale factors of 0.20 and 1.66, respectively, but showed similar surface composition. Samples A6 and A3 exhibited similar mottle Thurstone scale factors of 2.49 and 2.50, respectively, but showed significant differences in C/Ca ratios.

### *Statistical analysis of mottle from the combined data set*

We combined the mottle ratings of the data sets from all four data subgroups. Using these Thurstone scale factors as a response, we performed a regression analysis using the four most significant of thirteen input variables from Table IV. We analyzed the data again using a critical coating solids range of 72–78% after visual inspection of the graphical output of the drying model. **Table VII** shows the sensitivity of the significant variables defined as the product of the regression coefficient of a variable with its range of values and coefficient of determination from both these analyses. Table IV gives the variable definitions. In both cases, the effect of binder type was comparable to that of the other drying variables.

Two variables were highly confounded to the significant variables listed above but did not improve the model. Delta T1 was confounded with delta T2, and maximum evaporation rate in the critical solids zone was confounded with the critical solids range. After the statistical modeling was complete, we substituted several other variables such as zone 2 temperature, zone 4 temperature, distance to the start of the critical solids range, and evaporation rate at the start of the critical solids range. No improvement in the model occurred by adding any of these variables.

We also did a factor analysis using linear combinations of the input variables that yielded results consistent with the regression analysis. In addition, we analyzed the data again using a critical solids range of 72–78%. Four resultant factors from the factor analysis were the following:

- Factor 1 relates to the harshness of drying in the critical solids zone.
- Factor 2 relates to the setting of the latex structure.
- Factor 3 relates to the sheet tem perature profile through the dryers.
- Factor 4 relates to coating speed.

The Eigen values relative variation explained by the model due to the different factors for factors 1 through 4 are 3.77, 2.75, 2.58, and 1.75, respectively.

The three most important singular variables in Table IV from the factor model were the maximum evaporation rate in the critical solids zone, delta T2, and latex. High correlations existed between the following variables: Delta T1 with Delta T2 and coating solids range with maximum evaporation rate, average evaporation rate, and evaporation rate at 25%. Results from the factor analysis were consistent with those obtained from the regression analysis.

### *Computer modeling*

Computer modeling provided a better understanding of the critical drying process parameters and translated the pilot coater results to the drying process of the mill. The theoretical curves consist of the calculated net evaporation rates and calculated sheet temperatures of the coating throughout the drying process plotted against the sheet path distance. We noted the air setpoint temperatures for each air flotation dryers by shading and show the FCC and SCC values in the figures discussed below.

**Figure 6** shows the theoretical results for runs A5 and A6. A5 exhibited significantly less mottle than A6 with Thurstone scale factors of 0.58 and 2.49, respectively. The drying profile for the first two air flotation dryers was identical for both runs. Within the critical drying zone initially defined as the region between the FCC and SCC, run A6 exhibited higher net evaporation rates and sheet temperatures compared with A5. The values for run A5 started to increase significantly toward the latter part of the critical drying zone in D4 toward a longer sheet path distance. Improved mottle therefore resulted even when the evaporation rate significantly increased toward the end of the critical drying zone. These data

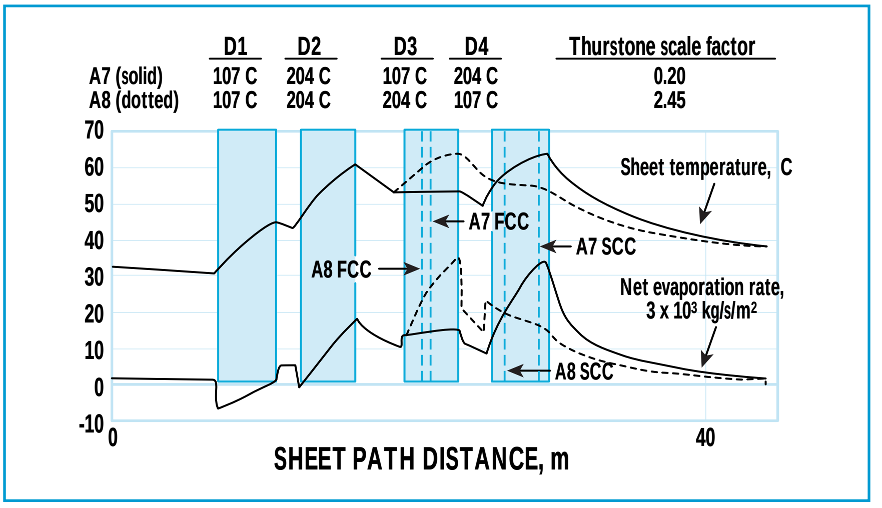


*7. Computer modeling results for A7 and A8*

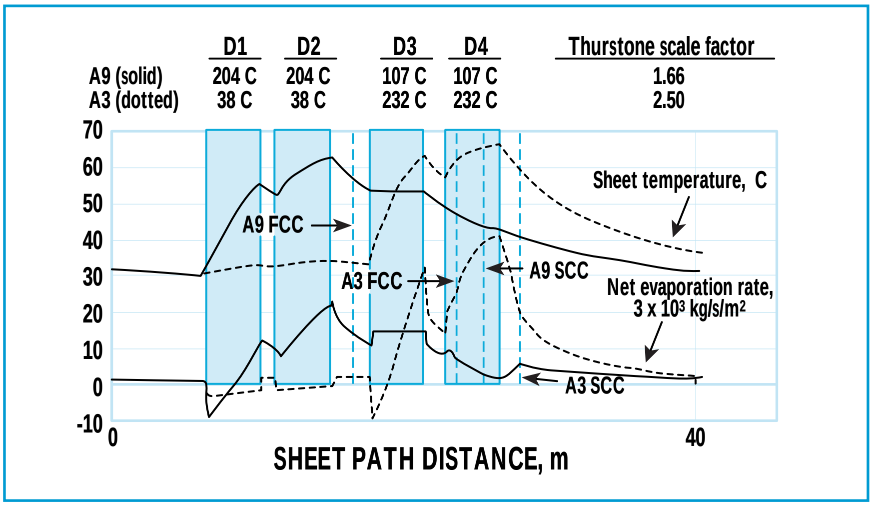


*8. Computer modeling results for A9 and A3*

suggest that this zone is narrower than the region bounded by the FCC and SCC. The critical drying zone seems defined by a coating solids range of 72–78% centered around 75%. In addition, a threshold of approximately 0.009 kg/sec/m$^2$ (7 lb/h/ft$^2$) for net evaporation rates occurred within this critical region. Severe mottle resulted above that point.

**Figure 7** shows the theoretical results for runs A7 and A8. They also exhibited significant differences in mottle with Thurstone scale factors of 0.20 and 2.45, respectively. Severe mottle again seems to relate to an evaporation rate above a threshold value within a narrow coating solids range. The drying profile for the first two air flotation dryers was also identical for both these runs. The D2 setpoint temperature was higher than runs A5 and A6. Before the critical drying zone, the net evaporation rate history therefore did not affect mottle.

**Figure 8** shows the theoretical results for runs A9 and A3. They exhibited significant differences in mottle with Thurstone scale factors of 1.66 and 2.50, respectively. Run A3 represented a harsh-late drying profile and had the largest increase from the D2 to D3 air setpoint temperatures of all the drying profiles used. Runs A9 and A3 represented extreme drying profiles used for all three coatings. Similar profiles resulted with coatings B and C. The results shown in Figs. 6–8 as discussed below were therefore representative of all the coatings.

**Figure 9** shows the theoretical and actual sheet temperature measurements for run A2. It had the following drying profile: 149°C, 149°C, 149°C, and 149°C for D1 through D4 air setpoint temperatures. A2 represented a moderate drying profile and was the only run with equivalent air setpoint temperatures for all the dryers. The measured sheet temperatures significantly increased within the region bounded by the FCC and SCC.

### *Other end-use properties*

Drying conditions over the range covered in this study did not significantly affect coating appearances or other end-use properties except porosity and percentage of drop using the K&N Labs test in a few cases. This was true even for coatings formulated with latexes conducive to binder migration—high glass transition temperature and small particle size.

## DISCUSSION

Our results show that drying strategy and choice of latex binder in the coating formulation significantly influenced mottle. We successfully translated the regression results to practical application at a mill to reduce mottle. The following methodology was a starting point:

- Determining the critical dryer that was approximately located in the critical drying zone
- Measuring web temperatures before and after this critical dryer
- Reducing evaporation rates in this critical dryer with adjustment of processing conditions to control the web temperatures so the exit temperature was lower or similar to the entering web temperature
- Decreasing the target coating speeds to lengthen the immobilization zone.

This methodology and the use of coating C have reduced mottle issues at the mill.

**Figure 10** shows profiles of evaporation and sheet temperature with drying time. Minimal drying occurs during the preheated phase where most of the energy transferred goes to heating. With application of additional heat, the web will experience a decline in the rate of temperature increase. This causes a corresponding rise in the rate of evaporation. The evaporation rate reaches a maximum during the steady state of evaporation phase. As the evaporation rate declines, sheet temperatures increase.

The FCC and SCC structural parameters relate approximately to the start of the steady state and falling rate of evaporation phases of the drying process, respectively *(10, 28)*. The FCC probably represents a solids concentration below which high intensity drying can safely be used without adversely affecting print quality. The SCC probably represents the completion of coating immobilization beyond which the sensitivity of the coating to evaporation rate is low. FCC and SCC therefore associate qualitatively with the range of the critical drying zone.

Our results suggest that the FCC occurs further along the drying profile than the start of the steady state of evaporation phase as generally believed. The data in Figure 9 indicate that the sheet temperatures from run A2 with a drying profile of equivalent air setpoint temperatures for all driers significantly increased within the region bounded by the FCC and SCC. The FCC is therefore probably closer to the end of the steady state of evaporation phase near the falling evaporation rate zone. The computer modeling results for other run conditions also support this conclusion. The degree of mottle is very sensitive to drying conditions near the FCC.

Our results agree with the consensus that the best drying strategy is reduction of the drying rate in a critical solids zone followed by hard drying after the critical zone. The key issue is a precise definition and determination

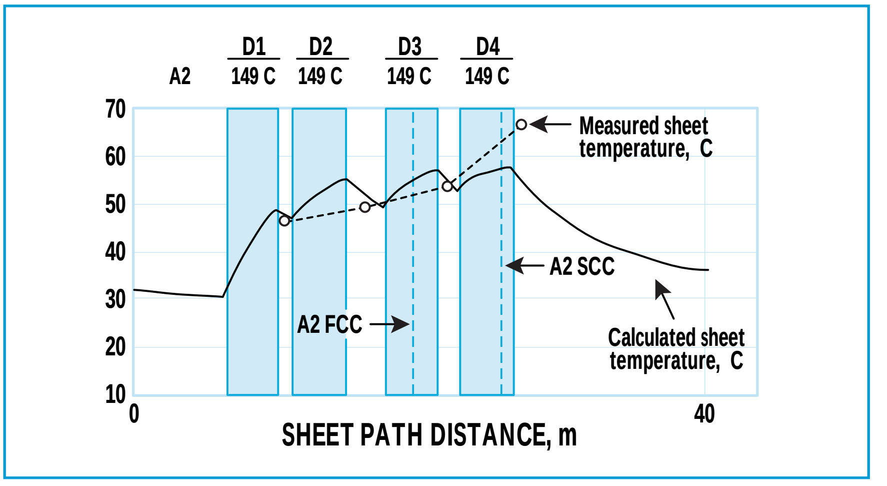


*9. Drying profile*

of the critical zone. Our modeling data show that the critical drying region associates with a narrow coating solids range of 72–78%. This critical drying region is narrower than that bounded by the FCC (74%) and SCC (84%) for coatings A and C and 82% for coating B. These results indicate that the calculated critical drying zone centers around the FCC. The threshold net evaporation rate within this narrow region is 0.009 kg/s/m$^2$ (7 lb/h/ft$^2$) by definition. Severe mottle results above this region. If these net evaporation rates were ≤ 0.007 kg/s/m$^2$ (5 lb/h/ft$^2$), the least amount of mottle resulted.

The best description of the effect of drying conditions on mottle uses the coating solidification process rather than defining optimum drying conditions by an energy input parameter. A possible explanation for the propensity to mottle from severe drying conditions at the FCC comes from consideration of the coating consolidation mechanism that **Fig. 11** shows. The coating consists of two different coating layers *(29, 30)*. One is a high solids filter cake at the coating immobilization solids that lies near the FCC. The other is a lower solids liquid coating layer near the application solids. We assume a small transition zone between these two layers instead of a more gradual solids gradient across the coating layer. The filter cake progressively grows in thickness as the coating continues to lose water until it reaches the air coating interface. At that point, a free liquid layer no longer exists. The evaporation rate of the coating should probably decrease. The liquid phase of the coating is still very mobile and can lead to redistribution of the coating constituents depending on the relative rates of evaporation and transport of liquid to the coating surface.

We could experimentally scrape off some coatings before the third air flotation dryer indicating the existence of a mobilized layer or liquid coating layer as shown above. Immobilization of the coatings occurred sometime within the third air flotation dryer, since we could not scrape off any coating after this dryer. As shown earlier, data in Fig. 9 indicates that the third dryer encompasses some falling rate of evaporation phase. The key to controlling mottle is to avoid harsh drying conditions at the early stages of the falling evaporation rate phase to avoid exceeding a critical threshold net evaporation rate. With extremely high evaporation rates severe enough to cause turbulent convection currents, disruption of the coating structure randomly at this point could induce surface nonuniformity and result in the transport of fluid phase components to areas where they were not originally distributed. This effect would also depend on localized regions of thicker coating

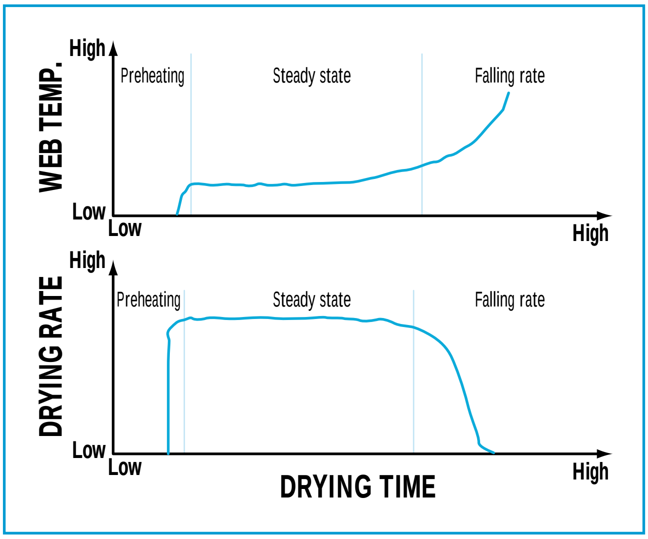


*10. Coating consolidation mechanism*

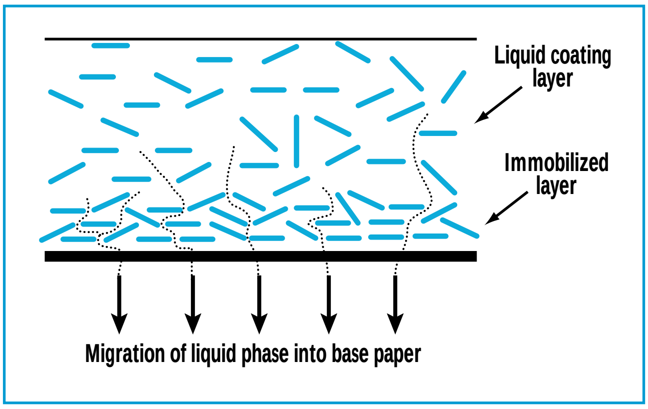


*11. Calculated and actual sheet temperature measurements for run A2 with shaded areas representing air flotation dryers D1–D4*

| Variable | Effect on back-trap mottle |
|---|---|
| Drying strategy | Significant |
| Binder type | Significant |
| Coating weight | Insignificant |
| IR drying and coating speed | Insignificant |

Insignificant ratings used a limited number of runs.

*VIII. Effect of variables on back-trap mottle*

within surface depressions of the basestock. This could exacerbate surface nonuniformity that is conducive to mottle. The disruption probably depends on the ratio of the energy input to the amount of water remaining in the coating structure.

The consolidation of a paper coating during drying is a complex process during which a substantial reduction of thickness can occur with considerable redistribution of the coating components. Vanderhoff and Bradford suggested consideration of convection or surface tension-driven currents that arise in the film at a critical stage of drying causing migration of small particles and resulting in an uneven distribution of latex particles *(31)*. They proposed that clay platelets become immobilized at a stage of drying where some small latex particles are still free to move. The conditioning phase refers to a reduced rate or stoppage of evaporation during the drying process—a mild-late condition. This allows the aqueous phase of the bulk coating layer to move in the surface pores to the coating surface where binder enrichment results. In a harsh-late drying profile, less binder probably goes to the coating surface where water evaporation and binder deposition could take place because the evaporation rate will be higher than the transport rate in the pores.

In our study, we used different drying profiles to induce different binder distributions throughout the coating to evaluate its effect on mottle. SEM photomicrographs in Fig. 4 show that a sample with a higher and more uniform binder concentration at the coating surface exhibited less mottle than a sample that exhibited severe mottle. This agrees with earlier work (*13, 32, 33*). These results indicate that binder enrichment in the coating surface as such cannot be the sole cause of mottle. Mechanisms have previously been proposed to explain this. These are an evaporation phase gap or conditioning phase in drying strategy *(34, 35)* as described above.

We also measured XPS data on the x-y surface uniformity of binder distribution besides the cross-sectional SEM data. Besides the extreme harsh-late drying condition, variation of drying profiles did not result in differences of the degree of surface component distribution determined by XPS. This suggests the existence of some mottle controlling parameter other than binder migration. Supporting this is data showing that mottle was the only end-use property that drying conditions significantly affected over the range covered in this study. In addition, the initial wet coating structure or its sensitivity to immobilization may relate with the susceptibility for mottle.

This parameter may relate to structure or some mechanism occurring just at or near the coating surface. Earlier work by others suggested consideration of a coating structure effect or something other than the binder distribution in the coating surface that relates to the mechanism for mottle *(13, 14)*. Engstrom and Rigdahl have postulated that a surface latex concentration may exist below which variation in surface porosity causes mottle *(35)*. Kline suggested that pore structure and surface binder concentration with some complex set of parameters may significantly affect print quality

KEYWORDS

*Adhesives, bibliographies, binders, coated papers, coatings, drying, ink, trapping, mathematical models, models, mottle, paper grades, print quality, process variables, properties, surface properties, variables.*

(16). Although the control and optimization of coating structure are necessary to achieve wet and dry coating strength required for offset printability, structure on a different scale or another mechanism may play an important role in reducing mottle.

## SUMMARY AND CONCLUSIONS

The primary objective of this study was identification of the critical drying process parameters at a mill to reduce back-trap mottle. We studied the impact of drying strategy, binder type, coating weight, and infrared drying and coating speed on the susceptibility to back-trap mottle. We applied coatings onto a 112 g/m$^2$ (74 lb/ream) wood-free basestock on a pilot coater that had air flotation and infrared dryers but not dryer cans. Computer modeling translated the pilot coater results to the drying process of a mill. Variation of drying strategy and its relationship to back-trap mottle showed the following results:

- Drying strategy and the choice of binder in the coating formulation significantly influenced back-trap mottle as **Table VIII** shows. No consistent trends related coating weights of 19 g/m$^2$ (13 lb/ream and 13 g/m$^2$ (9 lb/ream)), infrared drying, and coating speed to back-trap mottle using the limited data in our runs.
- Statistical analysis of back-trap mottle rankings provided numerical ratings that allowed computer modeling and regression analysis. We obtained predictive equations for target back-trap mottle values with the following significant variables: maximum evaporation rate within the critical solids zone, binder type, and change in sheet temperature between the second and third air flotation dryers. Translation of the regression results to practical application at a mill successfully reduced back-trap mottle.
- Theoretical results agreed with the work of others showing a required balance between a harsh-early and mild-late drying strategy and restricted net evaporation rates within a specific solids range to reduce back-trap mottle. Quantification of a threshold net evaporation rate within a narrow range coating solids of approximately 72–78% gave 0.009 kg/s/m$^2$ (7 lb/h/ft$^2$). Above this value, severe back-trap mottle resulted.

  The calculated critical drying zones were narrower than the region bounded by the FCC and SCC. Computer modeling results also showed the calculated critical drying zones centered around the FCC. The FCC is probably located closer to the start of the falling rate of evaporation phase of the drying process rather than the start of the steady state of evaporation phase as generally believed. The degree of back-trap mottle is highly sensitive to drying conditions right at the FCC. High evaporation rates at this point may cause sufficient disruption to produce nonuniform surface conditions conducive for back-trap mottle.
- SEM, XPS, and cryo-SEM data indicated that improved back-trap mottle resulted from a more consistent and higher binder concentration at the coating surface, a more consistent distribution of the surface components of a coating, and a more consistent distribution of wet state microstructure. Drying conditions over the range covered in this study did not significantly affect coating appearances or other end-use properties except porosity and percentage K&N drop in a few cases. This was true even for coatings formulated with latexes prone to binder migration high glass transition temperature and small particle size.

Future work will focus on further understanding of the mechanistic effect of drying conditions on the consolidation process to improve the ability to control operating conditions of dryers to reduce back-trap mottle and tailor binder modification. TJ

*Kim is senior research engineer, Pollock is development associate, Wittbrodt is research associate, Roper is research associate, and Smith is development leader at The Dow Chemical Co., 1604 Bldg., Midland, MI 48674. Stolarz is manager of product innovation, Rolf is manager of information development systems, Green is research fellow, and Langolf is senior product development engineer at Mead Corporation, P. O. Box 2500, Chillocothe, OH 45601.*

*Acknowledgements: The authors acknowledge and thank TEC Systems for access to their coating drying model. The simulation generated drying parameters used in the analysis of the pilot coater runs. The authors also thank Jeff McCoy, Joan Marshall, and David Hawn for their contributions and expertise in analytical support. Thanks also go to Jim Galloway, Ron VanGilder, Bruce Blom, Charles Kan, Pekka Salminen, Do Ik Lee, and Jim Beer for helpful discussions and to Brandon Hill for data translation of the computer modeling results.*

*Received Feb. 5, 1997.*
*Accepted April 8, 1997.*

*Presented at the TAPPI 1997 Coatings Conference.*

LITERATURE CITED


1. Dappen, J., *Tappi* 34(7):324(1951).
2. Heiser, E. J. and Cullen, D.W., *Tappi* 53(9):1739(1970).
3. Hultman, J. D., Leekley, R. M., and Garey, C. L., *Tappi* 60(11):105(1977).
4. Voss, H. and Garber, W. E., *Tappi* 58(9):99(1975).
5. Bergomi, J. G., Jr., *Tappi* 51(11):496(1968).
6. Sinclair, D., *Tappi* 50(8):424(1967).
7. Van der Kruk, H., *TAPPI 1989 Coating Conference Proceedings*, TAPPI PRESS, Atlanta, p. 199.
8. Aschan, P., *TAPPI 1986 Coating Conference Proceedings*, TAPPI PRESS, Atlanta, p. 73.
9. Norrdahl, P., *TAPPI 1991 Coating Conference Proceedings,* TAPPI PRESS, Atlanta, p. 41.
10. Hagen, K., in *Binder Migration in Paper and Paperboard Coatings* (M. J. Whalen-Shaw, Ed.), TAPPI PRESS, Atlanta, 1993, pp. 39–59.
11. Hirabayashi, T., Suzuki, H., Fukui, T., *et al.*, *TAPPI 1995 Coating Conference Proceedings*, TAPPI PRESS, Atlanta, p. 247.
12. Engstrom, G., Perrson, A., Fineman, I., *et al., TAPPI 1982 Coating Conference Proceedings,* TAPPI PRESS, Atlanta, p. 109.
13. Engstrom, G., Strom, G., and Norrdahl, P., *Tappi J.* 70(12):47(1987).
14. Engstrom, G., Rigdahl, M., Kline, J., *et al., Tappi J.* 74(5):171(1991).
15. Lazaroff, C. L., *TAPPI 1995 Coatiing Conference Proceedings,* TAPPI PRESS, Atlanta, p. 499.
16. Kline, J. E., *TAPPI1990 Coating Conference Proceedings,* TAPPI PRESS, Atlanta, p. 201
17. Yamazaki, K., Nishioka, T., Yoshihiko, H., *et al., Tappi J.* 76(5):9(1993).
18. Sandas, S. E., Salminen, P. J., and Eklund, D. E., *Tappi J.* 72(12):207(1989).
19. Thurstone, L. L., *Psychological Review* 34:273(19270.
20. Thurstone, L. L., *The Measurement of Values*, The University of Chicago Press, Chicago, 1959, pp. 67–81.
21. Sheehan, J. G. and Whalen-Shaw, M., *Tappi J.* 73(5):171(1990).
22. Watanabe, J. and Lepoutre, P., *J. of Applied Science* 27(11):4207(1982).
23. Arai, T., Yamasaki, T., Suzuki, K., *et al., Tappi 1988 Coating Conference Proceedings,* TAPPI PRESS, Atlanta, p. 187.
24. Arai, T. and Tomimasu, H., *Japan TAPPI*, 43(2):55(1989).
25. Engstrom, G., Norrdahl, P., and Strom, G., *TAPPI 1987 Coating Conference Proceedings,* TAPPI PRESS, Atlanta, p. 35.
26. Fukiwara, H. and Kline, J. E., *TAPPI 1986 International Process and Materials Quality Evaluation Conference Proceedings*, TAPPI PRESS, Atlanta, p. 157.
27. Brungard, N. L. and Cleland, A. J., *TAPPI 1994 Coating Conference Proceedings*, TAPPI PRESS, Atlanta, p. 13.
28. Engstrom, G. and Rigdahl, M., *Nordic Pulp and Paper Research Journal* 7(2):55(1992).
29. Letzelter, P. and Eklund, D., *Tappi J.* 76(5):63(1993).
30. Eriksson, U. and Rigdahl, M., *J. of Pulp and Paper Science* 20(11):J333(1994).
31. Vanderhoff, J. W. and Bradford, E. B., *TAPPI 1972 Coating Conference Proceedings*, TAPPI PRESS, Atlanta, p. 173.
32. Arai, T., Yamasaki, T., Suzuki, K. I., *et al., TAPPI 1988 Coating Conference Proceedings*, TAPPI PRESS, Atlanta, p. 187.
33. Fujiwara, H., Fujisaki, N., Shimizu, I., *et al.*, *TAPPI 1989 Coating Conference Proceedings*, TAPPI PRESS, Atlanta, p. 121.
34. Aschan, P., *Tappi* 61(12):35(1978).
35. Engstrom, G. and Rigdahl, M., in *Binder Migration in Paper and Paperboard Coatings* (M. J. Whalen-Shaw, Ed.), TAPPI PRESS, Atlanta, 1993, pp. 61–85.